Journal of the Chinese Chemical Society, **1993**, *40*, 509-516

Catalytic Properties of Layered and Pillared Buserite

She-Tin Wong (王志龍) and Soofin Cheng* (鄭淑芬)
Department of Chemistry, National Taiwan University, Taipei, Taiwan, R.O.C.

The catalytic properties of Na-buserite and Keggin ion-pillared buserite (abbreviated as KPB) in the oxidation of ethane, were investigated with varied mixtures of ethane and air. Na-buserite $Na_4Mn_{14}O_{26}{\cdot}xH_2O$ is a layered manganese oxide, KPB was prepared by the introduction of aluminium Keggin ions, $[Al_{13}O_4(OH)_{24}(H_2O)_{12}]^{7+}$ into the interlayers. Pillaring of the interlayers increases the active surface area participating in the reactions, as indicated by greater conversion over KPB than over a Na-buserite catalyst. In an oxygen-rich environment, complete combustion of ethane is achieved at temperatures ≈ 350 °C over KPB, and the structure of KPB is retained. The structure of KPB is less stable than that of Na-buserite in an oxygen-poor environment, and it disintegrates at large conversion. This phenomenon is explained in terms of the oxygen deficiency in the interlayer at a large reaction rate. Similar effects were absent from an oxygen-rich environment. The variation of the product selectivity of Na-buserite and KPB catalysts is discussed in terms of the presence of interlayer reaction sites.

INTRODUCTION

Na-buserite is a non-stoichiometric manganese oxide, formulated as $Na_4Mn_{14}O_{26}{\cdot}xH_2O$.[1-2] The non-stoichiometric nature of the oxide implies that the surface may contain chemically reactive oxygen.[3] Todorokite, nsutite and Na-buserite form the major components of manganese nodules that occur abundantly in both marine and fresh-water sediments. Manganese nodules are proved as effective as some commercial catalysts and adsorbents in reactions such as oxidation, reduction, decomposition and demetallation.[3] Therefore Na-buserite can be a cheap source of catalyst and catalyst support in the near future.

Na-buserite has a layered structure with edge-sharing MnO_6 octahedra.[4-5] The interlayer free spacing of dehydrated Na-buserite is about 1.9 Å, i.e. the diameter of the interlayer Na^+ ions. This small interlayer spacing precludes most reactions from occurring in the interlayers. The layered structure is thermally stable under 500 °C in both oxidative and reductive environments.[5] In order to improve the thermal stability and the active surface area, aluminium Keggin ions, of formula $[Al_{13}O_4(OH)_{24}(H_2O)_{12}]^{7+}$, are introduced into the interlayers. This introduction can be done successfully via hexylammonium ion-expanded buserite.[5] As the Keggin ion has a diameter about 8.6 Å,[6,7] its presence greatly improves the accessibility of the interlayers. The Keggin-ion pillar is stable to temperatures greater than 500 °C in air.[8] The Keggin ion-pillared buserite (abbreviated as KPB) prepared is stable at temperatures greater than 600 °C in both oxygen and nitrogen environments.[5]

Whereas various pillaring procedures were developed to convert densely layered metal oxides into microporous materials of high surface area, little work is reported on their catalytic behaviours.[9-15] Our objective was to examine the catalytic properties of Na-buserite and KPB samples in the oxidation of ethane. The results provide understanding of the local environment of the active sites in the catalytic reactions.

EXPERIMENTAL SECTION

In the preparation of KPB from Na-buserite, hexylamine was used as a swelling agent, and buserite expanded with hexylammonium ion was then used for the ion-exchange reaction with the aluminium Keggin-ion solution. The residual hexylammonium ions in the product were removed by calcination at 300 °C. Further details on the pillaring procedure are published.[5]

Powder X-ray diffraction (XRD) patterns were obtained on an automated powder diffractometer (Philips PW 1840), employing Ni-filtered Cu Kα radiation. BET surface areas were measured volumetrically with N_2 as adsorbate. Oxidation-reduction behaviours of the catalysts were studied on a thermogravimetric analyzer (Du Pont 951 TGA), with a heating rate 10 °C/min. The flow rates used were ≈ 100 mL/min except for ethane, which was 23 mL/min.

In catalytic experiments in which a small conversion

Dedicated to Professor Fa-Ching Chen (陳發清) on the occasion of his eightieth birthday.

was intended, Na-buserite or KPB sample (≤ 0.05 g) was diluted with SiO_2 (≈ 0.2 g) before use. The sample was pretreated at 370 °C in an air flow with an inlet flow rate 16 mL/min overnight. The molar fraction of air in the reactant mixture of ethane and air was fixed at 66.7 (oxygen-poor) and 99.4% (oxygen-rich), and the reaction was carried out at temperatures in the range 200 - 370 °C. The products were analyzed both on- and off-line by gas chromatography (GC) with thermal conductivity detector (TCD) facility. The reactor effluent from oxidation of ethane in an oxygen-deficient environment was monitored continuously with a quadrupole mass spectrometer (Thermolab 300D).

The ethane reactant stream was purified through a molecular sieve trap, and GC analysis showed that the proportion of impurity ethene was negligible. No CO_2 was detected.

Carbon analysis was done on an elemental analyzer (Perkin-Elmer 2400) with an accuracy 0.3%.

RESULTS

BET surface areas and porosity

The BET surface areas of Na-buserite and KPB fresh catalysts are 57 and 142 m^2/g, respectively. The porosity of the catalysts was determined by N_2 adsorption-desorption isotherms. The pillared compound showed an apparent increase in microporous condensation at a small partial pressure of N_2, and a slight hysteresis, which corresponds to a mesoporous structure. Typical isotherms of Na-buserite and KPB, pillared at 50 and 70 °C, are shown in Fig. 1.

Thermal stability of the catalysts

The thermal stability of Na-buserite and KPB catalysts under oxidation and reduction environments has been described separately.[5] Schemes I and II summarize the phase transformations of these two catalysts in gaseous environments of O_2, N_2 and H_2. Both catalysts are thermally most stable in oxygen and least stable in hydrogen. In an N_2 environment, Na-buserite decomposed into Mn_2O_3 and hollandite structures at about 373 °C, and Mn_2O_3 was further reduced to Mn_3O_4 at ≈ 529 °C. The reduction was accelerated when a mixture of H_2/N_2 (1:9) gas was used as carrier instead of N_2. In the presence of H_2, reduced phases of Mn_2O_3, Mn_3O_4 and MnO were observed at 282, 347 and 426 °C, respectively. In pure O_2 or air, Na-buserite was oxidized and formed $Na_2Mn_5O_{10}$ and cryptomelane at ≈ 560 °C. The structure of the pillared derivative KPB was stable until 600 °C in an environment of either N_2 or O_2. No oxygen uptake or disintegration of the structure was detected. Beyond these temperatures, the pillared structure collapsed and Mn_3O_4 (or Mn_2O_3) was formed from the buserite structure. In the environment of H_2, only the reduced phases of Mn_3O_4 and MnO were identified at 334 and 448 °C, respectively; the reduction of Mn_3O_4 to MnO is largely incomplete even at 600 °C.[5]

When Na-buserite was reduced under ethane with a

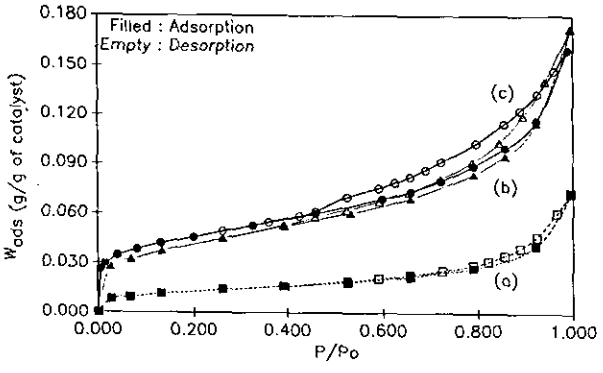

Fig. 1. Adsorption-desorption isotherms of N_2 on (a) Na-buserite, (b) KPB, ion-exchanged at 50 °C, and (c) KPB, ion-exchanged at 70 °C.

Scheme I Transformation of Na-buserite

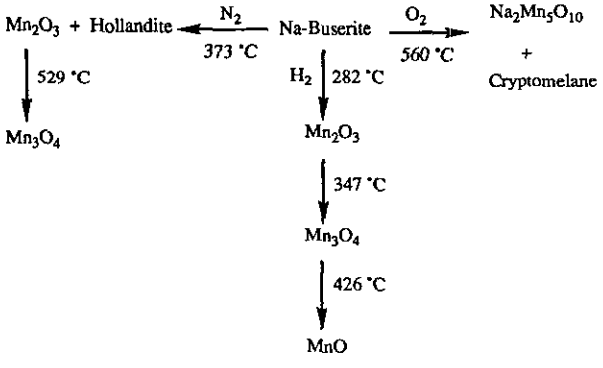

Scheme II Transformation of KPB

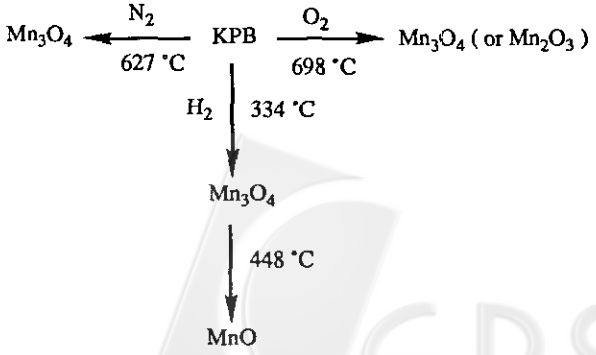

flow rate similar to that in the catalytic runs, the DTG profile showed two prominent peaks due to loss of weight at 383 and 592 °C; they are correlated with the formation of Mn_3O_4 and MnO, respectively. The peak due to the formation of Mn_2O_3 is less prominent, but can be observed at 260 °C. These results indicate that ethane acts as a reducing agent although its reducing power was not as great as that of hydrogen.

Oxidation of ethane

In this catalytic work, the conversion is defined as the fraction of ethane carbon converted to product carbon; for this calculation we assumed that coke formation on the catalyst surface is negligible, as was confirmed by carbon analysis of the used catalysts. In order to examine the catalytic behaviour and to characterize the active centre, the reaction was effected with varied proportion of oxygen.

(i) Oxygen-rich environment

The oxidation of ethane over Na-buserite and KPB catalysts was carried out with 99.4% of air in the reactant mixture. The contact period used is 1.5×10^{-4} g min mL^{-1}. The conversion over both catalysts varied insignificantly with duration on stream, except at the initial stages of reaction on the KPB catalyst. Fig. 2 shows the variation of conversion and selectivity over the KPB catalyst with duration on stream at 340 °C. The conversion decreased gradually with duration on stream, then reached a steady state after 6 h. In the case of Na-buserite catalyst, CO_2 was the only product at each reaction temperature, and also for KPB catalyst in the steady state except at 370 °C at which a minor proportion of CO was observed throughout the reaction (4 - 8%). In the initial stages of reaction, also ethene (340 & 370 °C) and CO (340 °C) were observed. According to Fig. 2, CO persisted to a longer duration on stream than ethene, and a maximum was observed for CO selectivity at the time that ethene selectivity was minimal.

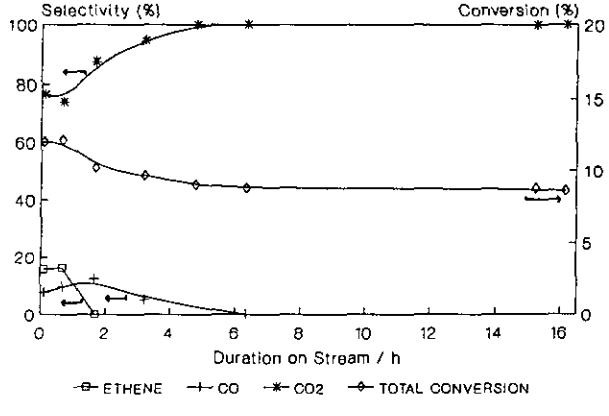

Fig. 2. Variation of selectivity and conversion with duration on stream over KPB catalyst in an oxygen-rich environment at 340 °C (contact period = 1.52×10^{-4} g min mL^{-1}).

The unit conversions for ethane oxidation over Na-buserite and KPB catalysts are compared in Fig. 3 at reaction temperatures 300, 340 and 370 °C. The unit conversion over KPB catalyst is greater than over Na-buserite at any reaction temperature.

Complete oxidation of ethane was intensified and nearly complete conversion was achieved over KPB catalyst at 350°C when the contact period was increased to 1.6×10^{-3} g min mL^{-1}.

(ii) Oxygen-poor environment

The oxidation of ethane over Na-buserite and KPB catalysts was carried out with 33 molar percent of air in the reactant mixture. Fig. 4 shows a typical plot of conversion versus reaction temperature over Na-buserite and KPB cata-

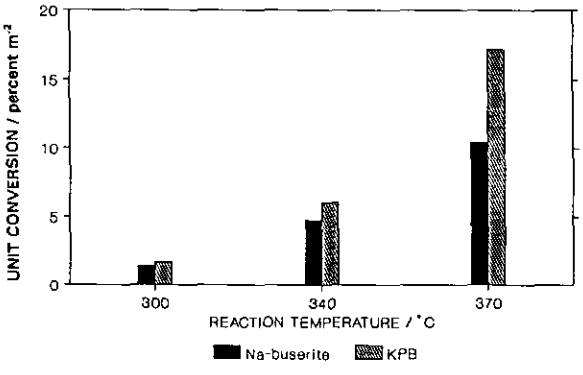

Fig. 3. Comparison of the unit conversion of Na-buserite and KPB catalysts in an oxygen-rich environment.

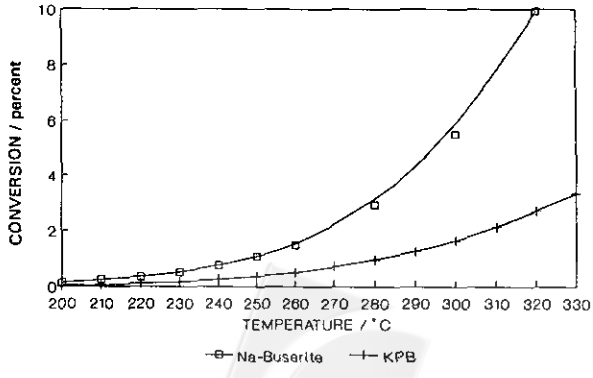

Fig. 4. Variation of conversion with reaction temperature over Na-buserite and KPB catalysts.

lysts, with fixed contact periods 4.3×10^{-3} and 5.8×10^{-4} g min mL^{-1}, respectively. The reaction temperature was varied in steps 10 or 20 °C. When the same contact period was used, the calculated conversion per unit area (percent/m^2) over KPB catalysts was slightly smaller than over Na-buserite, especially at reaction temperature ≥ 260 °C (Fig. 5). However, gradual deactivation was observed at temperatures ≥ 300 °C on both catalysts. For example, decreases of 20% (300 °C, after reaction period 17 h) and 15% (320 °C, after 8 h) were observed during the reaction for KPB and Na-buserite, respectively.

Fig. 6 shows a plot of ln (R_{obs}) versus 1/T; R_{obs} and T are the initial rate (s^{-1}) of ethane consumption and temperature (K) of reaction, respectively. The reaction temperature was varied between 200 - 320 °C. As the reactant concentration was kept constant, the activation energy (E_a) was calculated from the slope as 85 ± 5 kJ mol^{-1} for both catalysts. Under oxygen-rich conditions, a similar value (90 ± 5 kJ mol^{-1}) of E_a was obtained for the oxidation of ethane over KPB catalyst between 200 - 350 °C.

Fig. 7 shows the product selectivity as a function of conversion over both catalysts. The conversion over each catalyst was varied by altering the reaction temperature from 210 - 330 °C at a fixed contact period. CO_2 is the main product over Na-buserite even when the conversion is small (Fig. 7a). The ethene selectivity is small and CO selectivity is almost zero. Ethene and CO selectivities were observed in significant quantity over KPB catalyst (Fig. 7b).

Large alterations in the catalytic activities were observed at reaction temperatures 340 and 370 °C for KPB and Na-buserite, respectively. When the reaction temperature was increased from 300 to 340 °C, there was a greatly increased conversion over KPB catalyst to 16 - 17%. Based on the product yield, O_2 conversion approached 111% for KPB catalyst at this stage. Within about 8 h of reaction at 340 °C, the conversion decreased gradually with period on stream. However, the conversion decreased abruptly to 0.53% beyond that (Fig. 8). Regeneration in flowing air at 370 °C did not improve significantly the performance of this catalyst. In the case of Na-buserite, the catalytic activity was found to decrease at 370 °C, relative to that at 340 °C. The XRD patterns of these catalysts before and after catalytic oxidation of ethane appear in Fig. 10.

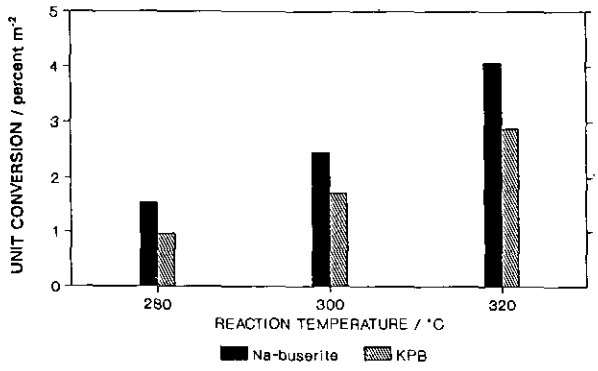

Fig. 5. Comparison of the unit conversion of Na-buserite and KPB catalysts in an oxygen-poor environment.

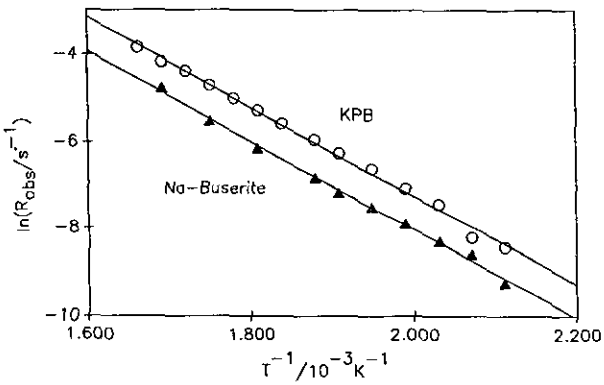

Fig. 6. Relationship between ln(R_{obs}) and 1/T.

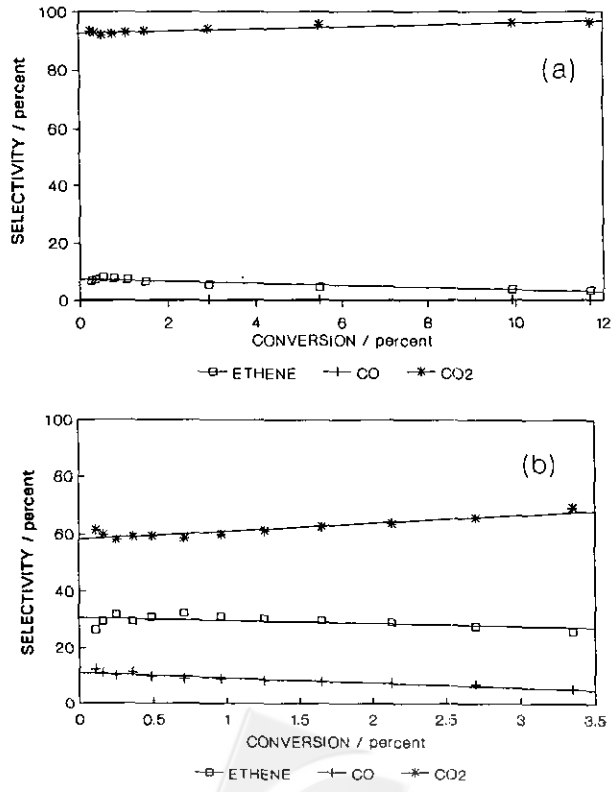

Fig. 7. Selectivity and conversion relationships over (a) Na-buserite, and (b) KPB catalyst, for an oxygen-poor environment.

The conversion of the catalysts carried out in various experiments were reproducible, within 6% deviation for Na-buserite and 10% for KPB. For Na-buserite, the selectivity of CO_2 and ethene at a given condition (conversion) was reproduced within 4% (separate batch of preparation) or 2% (same batch) of deviation. For KPB, only one preparation was chosen for the catalytic experiment, and the product selectivity was reproduced within 2% of deviation.

When a control catalytic run was carried out with SiO_2 as the catalyst, using a contact period 5.5×10^{-4} g min mL^{-1}, the results showed that SiO_2 is inert in ethane oxidation reaction. As to the partial oxidation product, ethene, the amount oxidized to CO_2 is negligible at 300 and 340 °C. At 370 °C, however, a maximum 11% of ethene formed in the reaction was converted to CO_2.

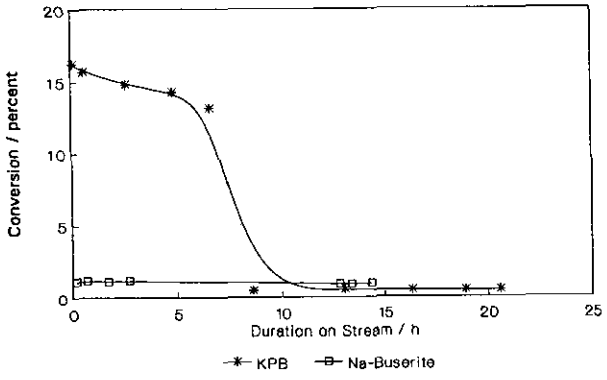

Fig. 8. Variation of conversion with duration on stream over Na-buserite and KPB catalysts in an oxygen-poor environment at 340 °C (contact period = 1.41×10^{-4} g min mL^{-1}).

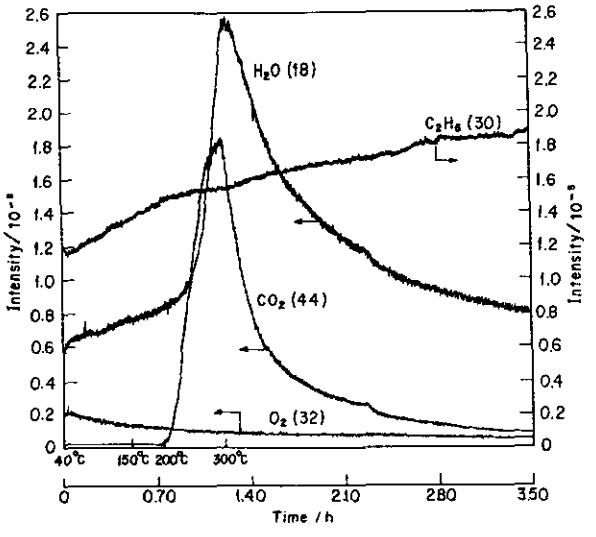

Fig. 9. Mass-spectrometric analysis of the reactor effluent from an oxygen-deficient environment.

(iii) Oxygen-deficient environment

The oxidation of ethane over Na-buserite in the absence of air was followed with a mass spectrometer. The reaction temperature was increased from 40 to 300 °C at a rate 5 °C/min, then held isothermally at 300 °C. Fig. 9 shows the variation of signal intensity with reaction duration for the reactant and product. CO_2 (mass/charge = 44) starts to appear after ≈ 40 min of reaction, which corresponds to a temperature of ≈ 190 °C, whereas the level of background oxygen (mass/charge = 32) remained nearly unchanged. Water (mass/charge = 18) also appeared in a similar range of temperature. The amount of ethane consumed in the reaction resulted in no perceptible alteration of the ethane signal intensity, due to the large excess of inlet ethane. The signals

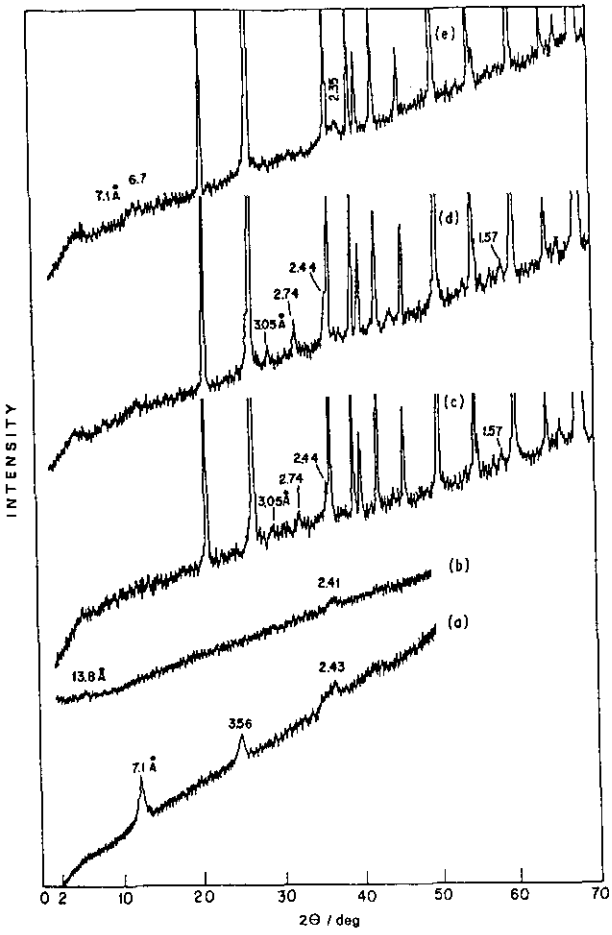

Fig. 10. XRD patterns of (a) Na-buserite (b) KPB (c) KPB, after reaction in an oxygen-poor environment at 340 °C (contact period = 1.41×10^{-4} g min mL^{-1}) (d) Na-buserite, after reaction in an oxygen-poor environment at 370 °C (contact period = 1.57×10^{-3} g min mL^{-1}), and (e) similar to (d) but with contact period = 1.41×10^{-4} g min mL^{-1}.

for ethene and CO were not identified separately, due to overlapping of the large signal from the ethane fragment (mass/charge = 28).

The conversion of ethane determined by GC is much smaller in an oxygen-deficient environment, than in either oxygen-poor or -rich environment. With a contact period 4.3×10^{-3} g min mL^{-1}, the results from GC analysis showed that the steady-state conversion was less than 0.05% at all temperatures. At the final stage of reaction at 320 °C, air was introduced into the ethane stream at the same molar ratio as in part (ii). The conversion increased to 7.3% within 7 min of reaction, and decayed gradually on stream (by 1.2% in 2 h). Water droplets deposited on the wall of the trap downstream. The reaction products were similar to that of part (ii), with 96% CO_2, 3% ethene and 1% CO.

Carbon analysis

Carbon analysis on as-synthesized samples of Na-buserite and KPB (after calcination in air at 300 °C for 2 h) showed that deposition of carbon was negligible on both samples during the preparation steps. On used catalysts, the carbon content was less than 0.3%.

Catalyst characterization

We measured the XRD patterns of Na-buserite and KPB catalysts before and after oxidation reactions in various oxygen contents to examine the structural change.

When oxidation of ethane was carried out under the oxygen-rich environment at reaction temperatures 300 - 370 °C, the structure of both KPB and Na-buserite used catalysts remained intact. However, in an oxygen-poor environment (Fig. 10), structural disintegration was observed at a large conversion. The diffraction peaks of the used catalysts are weak, because they were diluted with SiO_2 before use; these patterns of the used catalysts are therefore presented in an expanded form.

In the case of the fresh catalyst, the first diffraction peak was observed at d = 7.1 and 13.8 Å for Na-buserite and KPB catalysts, respectively (Figs. 10a & b). Figs. 10c and 10d are the diffraction patterns of the used Na-buserite and KPB catalysts after reaction at 370 and 340 °C, respectively. The structure of both catalysts disintegrated during ethane oxidation under the oxygen-poor environment. However, the reaction conditions for this to occur were more severe for Na-buserite. The peaks from fresh Na-buserite and KPB catalysts diminished and new peaks (besides SiO_2 peaks) were observed at d = 2.44, 2.74, 1.57 and 3.05 Å. Fig. 10e shows the XRD pattern of another used Na-buserite catalyst under the same reaction conditions as KPB catalyst in Fig. 10d. This catalyst deactivated directly at 370 °C without undergoing the process of structural disintegration. The XRD pattern of this catalyst shows peak at d = 7.1, 6.7 and 2.35 Å, besides SiO_2 peaks.

DISCUSSION

The interlayer free spacing of a dehydrated Na-buserite is about 1.9 Å. This spacing is too small for reactants to access, thus reactions occur exclusively on external surfaces. For KPB the interlayer free spacing is increased to 8.6 Å by the introduction of aluminium Keggin-ion pillars. Therefore, by comparing the catalytic data of KPB catalyst with that of Na-buserite, one can study the effect of the interlayer spaces in the KPB catalyst on the reaction.

For KPB catalyst, if the interlayer surface sites are freely accessible to the reactants and the active sites are distributed homogeneously as in the case of the external surface of Na-buserite, the conversion per surface area (unit conversion) and product selectivity would be comparable to that of Na-buserite under similar reaction conditions. This is however not the case observed here. The unit conversion over KPB catalyst in an oxygen-poor environment is slightly smaller than that of Na-buserite. The smaller unit conversion is unlikely due to coke formation in the interlayer during ethane oxidation, because the amount of carbon present in the used catalyst is negligible. Both KPB and Na-buserite have similar activation energies in this reaction. Therefore, the smaller unit conversion on KPB is not attributed to limitation of diffusion occuring in the interlayer either. That the activation energies of both catalysts are similar indicates similar natures of active sites on KPB and Na-buserite. The reason for the smaller unit conversion is likely that aluminium Keggin-ion pillars have no contribution in catalytic activity although their surfaces are counted as part of the total surface area.

For oxidation of ethane in an oxygen-rich environment, the unit conversion for KPB was greater than that of Na-buserite. The unit conversion for KPB at 300 °C for example corresponds to a rate about 1.4×10^{-3} s^{-1}, compared with about 3.5×10^{-4} s^{-1} for Na-buserite. The greater rate of reaction in KPB is likely due to an effect of heat transfer. The heat produced during oxidation of ethane in an oxygen-rich environment is greater on KPB than on the Na-buserite catalyst. The excess heat if trapped in the porous sample may cause an increased rate of reaction.

The product selectivity of KPB catalysts in an oxygen-poor environment (C_2H_6 : O_2 = 1 : 0.42) revealed a mild oxy-

gen deficiency in the interlayer. In order to oxidize fully one mole of ethane, 3.5 mol of dioxygen is required. If the supply of dioxygen by diffusion into the interlayer active sites cannot meet the demand, especially at a large rate of reaction, less oxidized products are favoured under this condition. Thus, significantly greater ethene and CO selectivities were obtained over KPB than Na-buserite catalyst. In a sequential reaction pathway, this mild oxygen deficiency in the interlayer that restricts the further oxidation of C_2H_4 or CO does not affect the rate of ethane consumption. Accordingly, the calculated value of E_a, which was based on the rate of disappearance of ethane, was unaffected by oxygen deficiency.

When the interlayer of KPB was exposed to an extremely oxygen-deficient environment during the oxidation reaction, the most serious consequence was the reductive disintegration of the buserite layer structure to lower Mn oxides. This effect was observed when the rate of reaction over KPB catalyst in an oxygen-poor experiment was increased rapidly to 16.3% as the temperature was raised from 300 to 340 °C. Based on the results of Na-buserite, the expected conversion of ethane over the KPB catalyst at 340 °C was 2.86%. If ethane were completely oxidized to CO_2, the O_2 conversion would be ≈ 25%. Thus, the surfaces of KPB are not oxygen-deficient. The structure of Na-buserite remained intact under similar reaction conditions. Therefore, the reduction process that caused the disintegration of the KPB structure is likely to begin in the interlayer and results in the local collapse of the pillared structure, which leads to an increased active surface area and ease of accessibility to these sites. The correspondingly greatly increased conversion leads to further oxygen deficiency in other parts of the interlayer and the cycle becomes repeated. The oxygen conversion over 100% (111%) at this stage clearly indicates that the oxygen supply was totally consumed in the reaction in addition to some oxygen contribution from lattice oxygen. Accompanying the consumption of lattice oxygen, the ethene selectivity decreased also. Lattice oxygen is hence clearly involved in the formation of ethene. The KPB catalyst after structural disintegration showed a sudden deactivation at a longer duration on stream (Fig. 8), due to complete consumption of the reactive lattice oxygen with the formation of stoichiometric lower Mn oxides. XRD analysis on the used KPB (and Na-buserite) catalysts after structural disintegration showed the presence of Mn_3O_4.

Na-buserite required more severe conditions to disintegrate its structure i.e. a much greater contact period at 370 °C. Under these conditions, the calculated conversion of O_2 was nearly 100%. This result is consistent with the suggestion above that reductive disintegration of the layered structure of buserite required an environment strongly deficient in O_2. With less severe conditions such as those used for the KPB catalyst, the structure of Na-buserite did not disintegrate, but deactivated directly. The cause of this deactivation may have been the thermal transformation of Na-buserite to Mn_2O_3 and hollandite, as the XRD pattern of the used catalyst is similar to that of Na-buserite heated in N_2 at similar temperatures.[5]

In an oxygen-rich environment, CO_2 is ultimately the favoured product on Na-buserite. In the case of KPB catalyst, oxygen deficiency products (CO and ethene) were also obtained at the initial stages of reaction at 300 and 340 °C. At 370 °C, the interlayer of KPB was slightly deficient in oxygen due to a greater consumption of oxygen at large conversions, and CO (ca. 4 - 8%) was produced throughout the reaction period.

As mentioned above, Na-buserite is a non-stoichiometric oxide. Reactions done on manganese nodules, such as decomposition of alcohol and oxidation of CO, showed that lattice oxygen was involved in the oxidation.[3] In addition, previous experiments on dehydrogenation of cyclohexane or cyclohexene on MnO_2 surface indicated that lattice O^{2-} was involved.[16,17] Therefore, the lattice oxygen is expected to act as the surface-reactive species responsible for dehydrogenation of ethane. From the results for an oxygen-deficient environment, the lattice oxygen was also found responsible for CO_2 formation. Thus the active sites in oxidation of ethane are probably lattice oxygen, and they are maintained by adsorption of oxygen in the reactant gas stream. Irreversible removal of the reactive lattice oxygen from the buserite structure leads to deactivation, and the eventual formation of lower Mn oxides. Moore et al.[18] have calculated the mass percentage of "active" oxygen in solid oxides and hydroxides of manganese that reacts with iron (II) ion; according to their method, the "active" oxygen was calculated as 15.0, 10.14, 7.0 and 0% for Na-buserite, Mn_2O_3, Mn_3O_4 and MnO, respectively. These values indicate that various Mn oxide species have varied content of reactive lattice oxygen, so to explain the variation in conversion observed for Na-buserite and its reduced phases.

However, other surface-adsorbed oxygen species, such as O^- and O_2^-, cannot be excluded from contributing to oxidation of ethane.[19] For example, O_2^- has been suggested to act as an active site during the dehydrogenation of 2-propanol on MnO_2 surfaces.[20]

From these results, the reaction sequence in the catalytic oxidation of ethane is proposed schematically as follows:

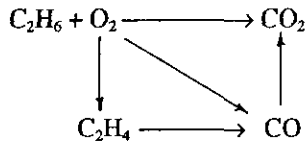

The byproduct, water, is omitted in this scheme. In an oxygen-poor environment, ethene, CO and CO_2 were observed even at small conversion. Therefore, they are likely formed through parallel pathways on the surface of Na-buserite and KPB catalysts. Dissociative adsorption of ethane was suggested to be the limiting step in the oxidation reaction.[21] As CO_2 is the predominant product over Na-buserite, the subsequent oxidation of adsorbed ethyl species to CO_2 is expected to proceed readily. However, in an oxygen-deficient environment, such as in the interlayers of KPB, the adsorbed ethyl species have a relatively greater tendency to form ethene and CO. The presence of a maximum for ethene and CO selectivities in Fig. 2, and the increased CO_2 selectivity as conversion of ethane increased in Figs. 7(a) and (b), indicate that the sequential oxidation pathway also occurs.

CONCLUSION

The KPB catalysts gave a greater conversion of ethane than Na-buserite in both oxygen-rich and -poor environments. Interlayer aluminium Keggin-ion pillars do not contribute to the activity in ethane oxidation; rather, the presence of these pillars increases the active surface area. In an oxygen-poor environment, reductive disintegration of both catalysts occurred at high conversion. KPB, which has a higher surface area, disintegrated under less severe reaction conditions than Na-buserite. Therefore, KPB and Na-buserite are suitable for catalytic oxidative reactions only in oxygen-rich environments in which their structures remain intact.

ACKNOWLEDGMENT

We thank the National Science Council of the Republic of China for financial support.

Received May 31, 1993.

Key Words

Na-buserite; Keggin ion-pillared buserite; Layered manganese oxide; Ethane oxidation.

REFERENCES

1. Giovanoli, R.; Buhler, H.; Sokolowska, K. *J. Microscopie* **1973**, *18*, 271.
2. Giovanoli, R.; Stähli, E.; Feitknecht, W. *Helv. Chim. Acta* **1970**, *53*, 209.
3. Nitta, M. *Appl. Catal.* **1984**, *9*, 151 and references therein.
4. Golden, D. C.; Dixon, J. B.; Chen, C. C. *Clays and Clay Minerals* **1986**, *34*, 511.
5. Wong, S. T.; Cheng, S. *Inorg. Chem.* **1992**, *31*, 1165.
6. Johansson, G. *Acta Chem. Scand.* **1960**, *14*, 769, 771.
7. Rausch, W. V.; Bale, H. D. *J. Chem. Phys.* **1964**, *40*, 3391.
8. Vaughan, D. E. W. *Catalysis Today* **1988**, 2, 187.
9. Landis, M. E.; Aufdembrink, B. A.; Chu, P.; Johnson, I. D.; Kirker, G. W.; Rubin, M. K. *J. Am. Chem. Soc.* **1991**, *113*, 3189.
10. Sprung, R.; Davis, M. E.; Kauffman, J. S.; Dybowski, C. *Ind. Eng. Chem. Res.* **1990**, *29*, 213.
11. Mehrotra, V.; Giannelis, E. P. *Chem. Mater.* **1992**, *4*, 20.
12. Johnson, I. D.; Werpy, T. A.; Pinnavaia, T. J. *J. Am. Chem. Soc.* **1988**, *110*, 8545.
13. Drezdon, M. A. *US Patent* 4,774,212, **1988**.
14. Clearfield, A.; Roberts, B. D. *Inorg. Chem.* **1988**, *27*, 3237.
15. Nazar, A. F.; Liblong, S. W.; Yin, X. T. *J. Am. Chem. Soc.* **1991**, *113*, 5889.
16. Basset, J. M.; Graydon, W. F. J. *Catal.* **1971**, *20*, 383.
17. Basset, J. M.; Vidaurre, A.; Graydon, W. F.; Praliaud, H. J. *Catal.* **1972**, *26*, 118.
18. Moore, T. E.; Ellis, M.; Selwood, P. W. *J. Am. Chem. Soc.* **1950**, *72*, 856.
19. Che, M.; Tench, A. J. *Adv. Catal.* **1983**, *32*, 1.
20. Hasegawa, S.; Yasuda, K.; Mase, T.; Kawaguchi, T. *J. Catal.* **1977**, *46*, 125.
21. Hiam, L.; Wise, H.; Chaikin, S. *J. Catal.* **1968**, *9*, 272.